Materials Letters 114 (2014) 26–28

Contents lists available at ScienceDirect

Materials Letters

journal homepage: www.elsevier.com/locate/matlet

Influence of the growth temperature of AlN nucleation layer on AlN template grown by high-temperature MOCVD

Yiren Chen [a,c], Hang Song [a,*], Dabing Li [a,*], Xiaojuan Sun [a], Hong Jiang [a], Zhiming Li [a], Guoqing Miao [a], Zhiwei Zhang [a], Yue Zhou [b]

[a] State Key Laboratory of Luminescence and Applications, Changchun Institute of Optics, Fine Mechanics and Physics, Chinese Academy of Sciences, Changchun 130033, People's Republic of China
[b] State Key Laboratory of Applied Optics, Changchun Institute of Optics, Fine Mechanics and Physics, Chinese Academy of Sciences, Changchun 130033, People's Republic of China
[c] University of Chinese Academy of Sciences, Beijing 100039, People's Republic of China

ARTICLE INFO

Article history:
Received 25 July 2013
Accepted 26 September 2013
Available online 4 October 2013

Keywords:
Epitaxial growth
Chemical vapor deposition
Semiconductors
Raman
AlN template

ABSTRACT

We studied the influence of the growth temperature of AlN nucleation layer (T_{NL}) on the AlN template grown by high-temperature metal-organic chemical vapor deposition (HT-MOCVD). The AlN templates were characterized by high-resolution X-ray diffractometer, atomic force microscopy and room-temperature Raman scattering spectrometer. The results revealed that the T_{NL} had a direct influence on the quality of the AlN template. By optimizing the T_{NL} at 950 °C, we obtained a high-quality AlN template with the full width at half maxima for the (0002) and (10–12) planes of 90″ and 612″, respectively. The AlN template also presented atomic level step with a root mean square (RMS) roughness of 0.133 nm. In addition, it performed excellent single crystallographic orientation along the *c*-axis. The growth evolution of AlN nucleation layer at different T_{NL} was also explained in detail.

1. Introduction

Aluminum nitride (AlN) single crystal is considered to be an ideal substrate for AlGaN-based deep ultraviolet optoelectronic devices [1–3] and [4], owing to its high thermal conductivity, wide band gap energy and excellent lattice matching with gallium nitride [5]. However, its applications are severely restricted by the size and price under the existing mainstream growth methods of solution growth [6] and sublimation–recondensation [7]. In order to overcome the disadvantages of bulk AlN substrate, the techniques of heteroepitaxial growth such as hydride vapor phase epitaxy (HVPE), metal-organic chemical vapor deposition (MOCVD) and molecular beam epitaxy (MBE) have been developed to prepare AlN template as the alternative. Sapphire is one of the most popular substrates for AlN template due to its low cost, wide availability in large diameter and stability at high temperature. However, the large lattice and thermal mismatch between AlN and sapphire lead to high-density of dislocations in the AlN template. In addition, poor surface migration of Al adatoms on sapphire deteriorates the morphology of AlN template severely [8]. These disadvantages have direct influences on the performance of AlGaN-based epilayers. Therefore, the preparation of high-quality AlN template on sapphire plays an important significance. Corekci et al. [9] have investigated the effect of ammonia (NH_3) flow rate and layer thickness on the properties of AlN template. And the influence of III/V flux ratio on the properties of AlN template also has been studied by Falth group [10]. However, the growth temperature of AlN nucleation layer (T_{NL}) is another important factor. In this paper, we studied the influence of T_{NL} on the quality of AlN template.

2. Experimental procedure

The AlN template samples were grown on 2 in. *c*-plane sapphire substrates by high-temperature metal-organic chemical vapor deposition (HT-MOCVD). Trimethyl aluminum (TMAl) and NH_3 were used as Al and N precursors, respectively. The two-step growth method was used as follows: first, the sapphire was thermally cleaned at 1100 °C under H_2 for 480 s. Subsequently, a 36-nm-thick AlN nucleation layer (NL) was deposited on sapphire. In order to understand the influence of T_{NL} on the crystalline quality of AlN template, the NLs were deposited at 880 °C, 950 °C and 1020 °C, corresponding to samples A, B and C respectively. After then, the growth temperature was ramped up to 1300 °C and the recrystallization of NL was carried out during the temperature-rise period. Finally, the high-temperature AlN (HT-AlN) was grown on NL at 1300 °C for 3800 s and the growth rate was calculated to be 0.99 μm/

* Corresponding authors. Tel./fax: +86 431 84627073.
E-mail address: songh@ciomp.ac.cn (H. Song).

0167-577X/$ - see front matter © 2013 Elsevier B.V. All rights reserved.
http://dx.doi.org/10.1016/j.matlet.2013.09.096

h by in situ monitoring system. The thickness of the HT-AlN was about 1.05 μm.

We used 405 nm in situ optical monitoring system (LayTec AG) during the growth of AlN templates by HT-MOCVD. The AlN templates were also characterized by atomic force microscope (AFM, Veeco multi-mode) and X-ray diffractometer (XRD, Bruker D8) using rocking curve scan. The Raman scattering spectra were recorded at room-temperature in backscattering geometry using the 488 nm line of an Ar^+ ion laser (LabRam Infinity) as the excitation source.

3. Results and discussion

As shown in Fig. 1, the relationship between T_{NL} and the full width at half maximum (FWHM) values of (0002) and (10–12) planes for the three samples was demonstrated. The FWHM values of (0002) plane were 306, 90 and 126″ while the values of (10–12) plane were 846, 612 and 702″, corresponding to samples A, B and C respectively. The FWHM values measured by XRD were widely used to estimate the dislocations in AlN template, mainly including screw and edge dislocations [11]. The screw dislocation density (ρ_s) and edge dislocation density (ρ_e) were evaluated by [12]

$$\rho_s = \beta_{(0002)}{}^2/(2\pi\ln 2 \times |b_c|^2),\ \ \rho_e = \beta_{(10-12)}{}^2/(2\pi\ln 2 \times |b_a|^2) \quad (1)$$

where $\beta_{(0002)}$ and $\beta_{(10-12)}$ were the FWHMs of (0002) and (10–12) planes, $\boldsymbol{b}_c$ and $\boldsymbol{b}_a$ stood for the Burgers vector lengths equated to *c*- and *a*-axial lattice constants, respectively. The ρ_s and ρ_e were calculated to be 2.04×10^8 cm^{-2} and 4.66×10^9 cm^{-2} for sample A, 1.76×10^7 cm^{-2} and 3.61×10^9 cm^{-2} for sample B, and 3.46×10^7 cm^{-2} and 4.51×10^9 cm^{-2} for sample C. In comparison, sample B performed highest quality.

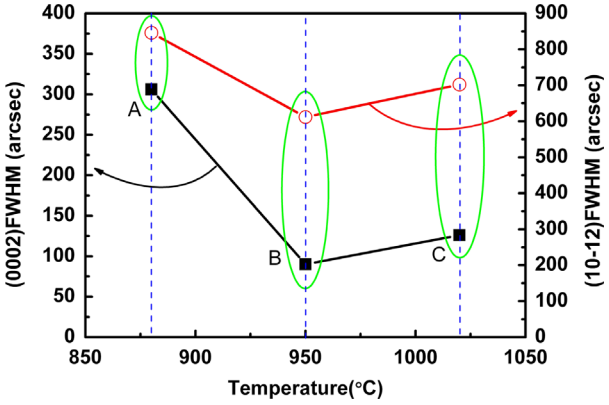

Fig. 1. The relationship between T_{NL} and FWHM values of (0002) and (10–12) planes of AlN templates.

Fig. 2(a) and (b) shows the short-wavelength (405 nm) in situ monitoring curve vs. time sequence of two-step growth of AlN and three-dimensional (3D) AFM images for the three samples. The reflectance was used to reveal the growth evolution of NL at different T_{NL}. The section (I) in all the reflectance curves is corresponding to NL growing, as shown in Fig. 2(a). The reflectance intensity was related to the roughness of NL which was determined by the grain density and size of 3D AlN islands. Thus, the reflectance intensities followed a sequence of A < B < C meant the roughness of NL decreased by increasing the T_{NL}. This result could be ascribed to the reason that the diffusion length of Al adatoms and lateral coherence length at sapphire surface was increasing while T_{NL} was increased [13]. We explained the growth evolution of AlN NL at different T_{NL} as follows.

For sample A, the normal growth rate was higher than that of lateral due to the poor mobility of Al adatoms on lateral direction, so a large density of big isolated 3D AlN islands deposited on sapphire. During the recrystallization, big isolated islands recrystallized to transform into columnar islands with great orientation difference. For sample B, because of the improvement of migration of Al adatoms, the density of isolated 3D AlN islands decreased while the grain size increased. As the growth time increased, the 3D AlN islands grew in both lateral and normal directions harmoniously, and formed islands with hexagonal-like vertebral

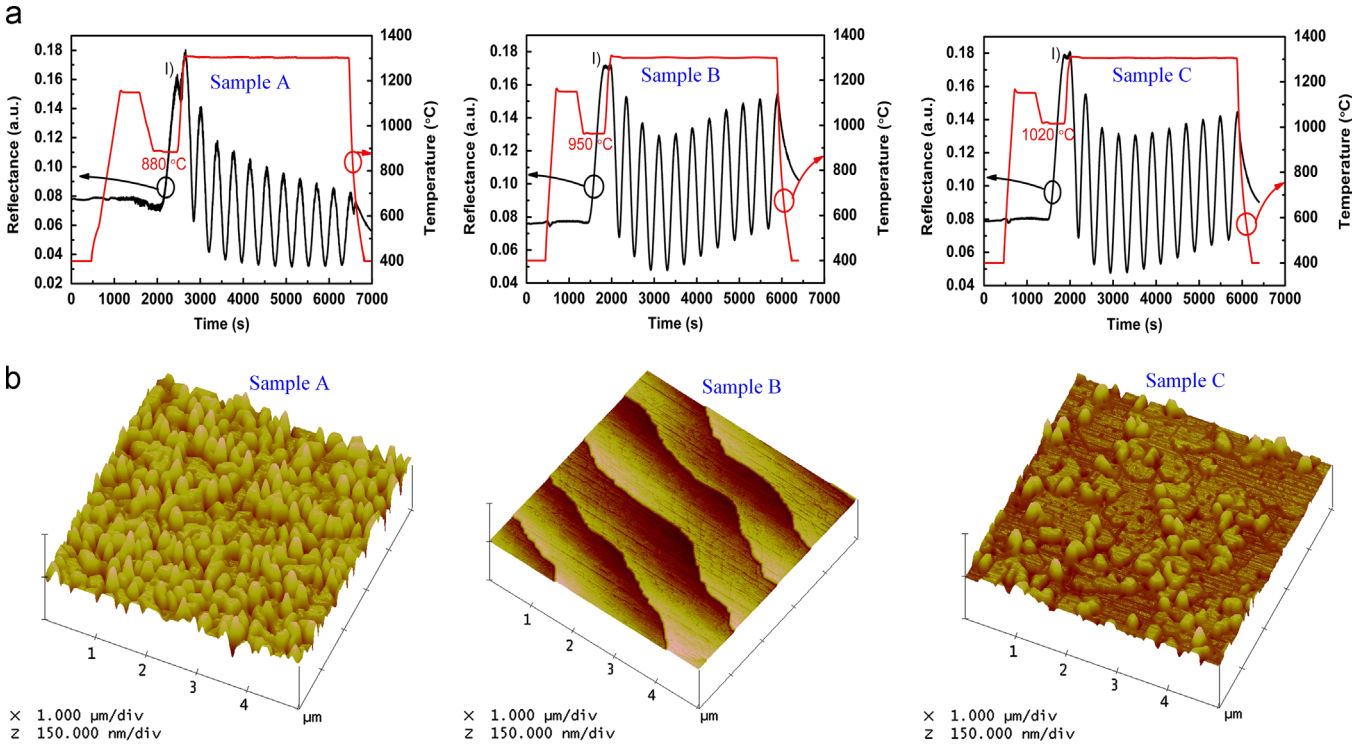

Fig. 2. (a) The 405 nm wavelength in situ monitoring curve vs. time sequence and (b) AFM images for samples A, B and C. The scan area of AFM image is 5×5 μm^2.

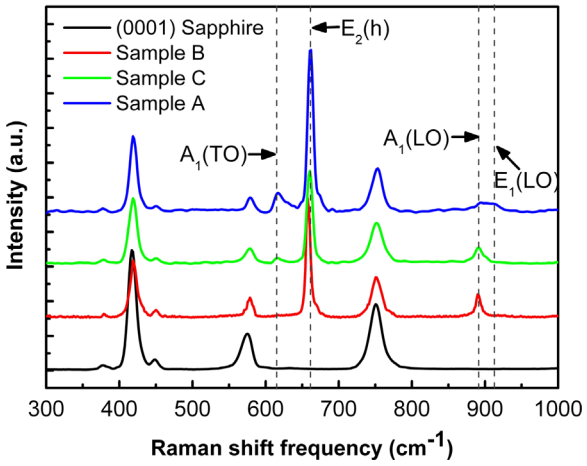

Fig. 3. The Raman spectra of *c*-axis AlN templates in accordance with different T_{NL}.

mesa which presented smaller roughness of NL than sample A. As to sample C, the fast diffusion of Al adatoms made the lateral growth dominant. The density of 3D AlN islands further decreased but the grain size further increased in contrast with sample B. The result made the 3D islands of AlN NL prematurely coalesced partially during the growth, and its surface morphology changed from islands with hexagonal-like vertebral mesa to a mixture of islands and two-dimensional (2D) planes. Once the surface morphology of NL was formed, the subsequent growth was dominated. After HT-AlN growth, sample B obtained a smooth surface with obvious atomic step as shown in Fig. 2(b). Its RMS roughness was of 0.133 nm. However, flat surface co-existence with some hillocks was observed in sample C while the surface morphology of sample A was rough with many hillocks.

The crystallographic orientations of three samples were also investigated by Raman spectroscopy. All measurements were carried out at normal incidence to the surface of samples. As shown in Fig. 3, excluding the peaks of *c*-plane sapphire, the peaks of sample B were located at the frequencies of 657.42 cm^{-1} and 889.928 cm^{-1}, corresponding to the E_2(h) and A_1(LO) phonon modes, respectively. The study had shown that only the non-polar E_2(h) and polar A_1(LO) modes were allowed for *c*-oriented wurtzite structure AlN [13]. And the unstrained phonon frequencies of AlN at room-temperature were 657.4 cm^{-1} and 890 cm^{-1} for E_2(h) and A_1(LO) modes [14]. Therefore, sample *B* presented excellent single crystallographic orientation along c-axis and almost strain-free. The Raman spectrum of sample *C* showed another active peak at 615.844 cm^{-1} which corresponded to A_1(TO) mode besides the E_2(h) mode and A_1(LO) mode (located at 660.49 cm^{-1} and 891.412 cm^{-1}, respectively). Usually, only the E_2 and A_1(LO) modes were allowed for the $z(yy)\bar{z}$ scattering configuration at normal incidence of excited laser along the *c*-axis. However, the existence of A_1(TO) mode which allowed for $y(zz)\bar{y}$ or $y(xx)\bar{y}$ configuration meant the disoriented crystallites of sample C. Distinguished from sample B and C, an additional E_1(LO) phonon mode (located at 912.159 cm^{-1}) which was allowed for $y(xz)\bar{x}$ configuration was measured in sample A. The observed phonon lines of sample A clearly indicated non-polar, semi-polar and polar orientations of crystallites.

4. Conclusions

We obtained high-quality AlN template by optimizing the growth temperature of AlN nucleation layer. The results disclosed that good crystalline quality of AlN template with smooth and uniform surface morphology, small FWHM values in both (0002) and (10–12) planes as well as coincident crystallographic orientation could be obtained by optimizing the T_{NL} at 950 °C. At the temperature, the 3D AlN islands of NL grew in both lateral and normal directions harmoniously which played an important role in preparing high-quality AlN template.

Acknowledgments

This work was partially supported by the National Key Basic Research Program of China (Grant No. 2011CB301901), the National Natural Science Foundation of China (Grant Nos. 61322406, 61274038, 61204070, 51072195 and 51072196), and the National High-Tech R&D Program (863, Grant No. 2011AA03A111).

References

[1] Sun Q, Kwon SY, Han J, Davitt K, Song YK, Nurmikko AV, et al. Applied Physics Letters 2007;91:051116.
[2] Kneissl M, Yang Z, Teepe M, Knollenberg C, Schmidt O, Kiesel P, et al. Journal of Applied Physics 2007;101:123103.
[3] Jiang H, Egawa T. Applied Physics Letters 2007;90:121121.
[4] Hu X, Deng J, Pala N, Gaska R, Shur MS, Chen CQ, et al. Applied Physics Letters 2003;82:1299–301.
[5] Matioli E, Brinkley S, Kelchner KM, Hu YL, Nakamura S, DenBaars S, et al. Light: Science and Applications 2012;1:1–7.
[6] Kangawa Y, Toki , Yayama T, Epelbaum BM, Kakimoto K. Applied Physics Express 2011;4:095501.
[7] Schlesser R, Dalmau R, Sitar Z. Journal of Crystal Growth 2002;241:416–20.
[8] Lobanova AV, Yakovlev EV, Talalaev RA, Thapa SB, Scholz F. Journal of Crystal Growth 2008;310:4935–8.
[9] Corekci S, Ozturk MK, Cakmak M, Ozcelik S, Ozbay E. Materials Science in Semiconductor Processing 2012;15:32–6.
[10] Falth JF, Davidsson SK, Liu XY, Andersson TG. Applied Physics Letters 2005;87:161901.
[11] Sun XJ, Li DB, Chen YR, Song H, Jiang H, Li ZM, et al. CrystEngComm 2013;15:6066–73.
[12] Lee SR, West AM, Allerman AA, Waldrip KE, Follstaedt DM, Provencio PP, et al. Applied Physics Letters 2005;86:241904.
[13] Balaji M, Claudel A, Fellmann V, Gelard I, Blanquet E, Boichot R, et al. Journal of Alloys and Compounds 2012;526:103–9.
[14] Davydov VYu, Kitaev YuE, Goncharuk IN, Smirnov AN, Graul J, Semchinova O, et al. Physical Review B 1998;58:12899–907.